Liquid Crystalline Perylene Diimides: Architecture and Charge Carrier Mobilities

Corien W. Struijk,[†] Alexander B. Sieval,[†] Jarno E. J. Dakhorst,[†] Marinus van Dijk,[†] Peter Kimkes,[†] Rob B. M. Koehorst,[‡] Harry Donker,[‡] Tjeerd J. Schaafsma, Stephen J. Picken,[§,||] Anick M. van de Craats,[⊥] John M. Warman,[⊥] Han Zuilhof,*[,†] and Ernst J. R. Sudhölter*[,†]

Contribution from the Laboratory of Organic Chemistry, Wageningen University, Dreijenplein 8, 6703 HB Wageningen, The Netherlands, Laboratory of Molecular Physics, Wageningen University, Dreijenlaan 3, 6703 HA Wageningen, The Netherlands, Akzo Nobel Central Research, Velperweg 76, 6800 SM Arnhem, The Netherlands, and Interfaculty Reactor Institute, Delft University of Technology, Mekelweg 15, 2629 JB Delft, The Netherlands

Received March 20, 2000

Abstract: The phase behavior of three *N*-alkyl-substituted perylene diimide derivatives is examined by differential scanning calorimetry and polarized optical microscopy. The occurrence of multiple phase transitions indicates several crystalline and several liquid crystalline phases. X-ray diffraction measurements show that the liquid crystalline phases display high structural ordering in all three dimensions: smectic layers are formed, and within these smectic layers an additional ordering in columns is observed. Molecular modeling confirms this result and substantiates smectic ordering with interdigitating alkyl chains that determine the distance between the smectic layers. The ordering in columns is favored by $\pi-\pi$ interactions between the cofacially oriented perylene molecules and by the elliptic shape of the molecule. Finally, intermolecular dipole−dipole interactions between the carbonyl groups of the imide moieties cause the perylene molecules to orient on average with a slight rotation between neighboring molecules within a columnar stack. Following the determination of the electronic transition dipole moment, this orientation, which still involves substantial $\pi-\pi$ interactions, could be confirmed by UV/vis spectroscopy of perylene aggregates. To gauge the potential of these materials as organic semiconductors, the charge carrier mobility of one of the perylene derivatives has been measured by pulse-radiolysis time-resolved microwave conductivity. A value in excess of 0.1 $cm^2\ V^{-1}\ s^{-1}$ is found in the liquid crystalline phase, and a value in excess of 0.2 $cm^2\ V^{-1}\ s^{-1}$ is found for the crystalline phase. These values are comparable with the highest values previously found for other discotic materials.

Introduction

Perylene derivatives are promising compounds for application in electronic devices as molecular semiconductors. Most organic conducting materials can be described as p-type semiconductors, in which holes in the valence band are the majority charge carriers. In contrast, in *N,N′*-dialkyl-3,4,9,10-perylenetetracarboxyldiimides the majority charge carriers are electrons in the conduction band, and this material is thus classified as an n-type semiconductor.[1,2] Such materials are potentially useful as the electron-accepting materials in all organic photovoltaic solar cells, as was reported in 1986 for the first solar cell based on a phthalocyanine and a perylenetetracarboxylic derivative.[3] This type of solar cell is based on a p−n junction in which the phthalocyanine is the p-type material (electron donor) and the perylene derivative is the n-type material (electron acceptor). Since then, much research has been done on this kind of solar cell,[4−11] but the energy conversion efficiencies are still limited to about 1%, as was, e.g., obtained for p−n junctions of zinc phthalocyanines (50 nm ZnPc) and *N,N′*-dimethyl-3,4,9,10-perylenetetracarboxyldiimides (25−50 nm PTCDI).[12] Ways to improve the efficiency of the p−n junction include an increase of the exciton diffusion length and an improvement of the transport of charge carriers in the organic material. Optimization of these aspects allows for the use of thicker light-absorbing layers, which has the effect that a higher percentage of the incident sunlight can be absorbed.

* To whom correspondence should be addressed. E-mail: Ernst.Sudholter@PHYS.OC.WAU.NL

[†] Laboratory of Organic Chemistry, Wageningen University.

[‡] Laboratory of Molecular Physics, Wageningen University.

[§] Akzo Nobel Central Research.

[||] Present address: Department of Materials Science and Technology, PEPM, Delft University of Technology, Julianalaan 136, 2628 BL Delft, The Netherlands.

[⊥] Delft University of Technology.

(1) Meyer, J.-P.; Schlettwein, D.; Wöhrle, D.; Jaeger, N. I. *Thin Solid Films* **1995**, *258*, 317−324.

(2) Horowitz, G.; Kouki, F.; Spearman, P.; Fichou, D.; Nogues, C.; Pan, X.; Garnier, F. *Adv. Mater.* **1996**, *8*, 242−245.

(3) Tang, C. W. *Appl. Phys. Lett.* **1986**, *48*, 183−185.

(4) Panayotatos, P.; Parikh, D. *Sol. Cells* **1986**, *18*, 71−84.

(5) Günster, S.; Siebentritt, S.; Meissner, D. *Mol. Cryst. Liq. Cryst.* **1993**, *229*, 111−116.

(6) Wöhrle, D.; Meissner, D. *Adv. Mater.* **1991**, *3*, 129−138.

(7) Gregg, B. A. *Chem. Phys. Lett.* **1996**, *258*, 376−380.

(8) Tsuzuki, T.; Hirota, N.; Noma, N.; Shirota, Y. *Thin Solid Films* **1996**, *273*, 177−180.

(9) Panayotatos, P.; Bird, G.; Sauers, R.; Piechowski, A.; Husain, S. *Sol. Cells* **1987**, *21*, 301−311.

(10) Siebentritt, S.; Günster, S.; Meissner, D. *Synth. Met.* **1991**, *41−43*, 1173−1176.

(11) Oekermann, T.; Schlettwein, D. R. A.; Wöhrle, D. *J. Appl. Electrochem.* **1997**, *27*, 1172−1178.

(12) Wöhrle, D.; Kreienhoop, L.; Schnurpfeil, G.; Elbe, J.; Tennigkeit, B.; Hiller, S.; Schlettwein, D. *J. Mater. Chem.* **1995**, *5*, 1819−1829.

10.1021/ja000991g CCC: $19.00
Published on Web 11/01/2000

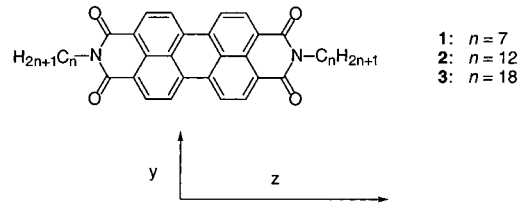

Figure 1. Structures of perylene derivatives.

Many different phthalocyanines[13] (and other electron-donating materials[14]) have already been synthesized and characterized, but the perylene part has received much less attention. It has been shown that increased ordering of the perylene derivatives in the presence of the vapor of an organic solvent leads to an increase in exciton diffusion length.[15] For an *N,N′*-bis(phenethylimide)-3,4,9,10-perylenebiscarboximide film, which has been annealed by exposure to methylene chloride vapor for 3 h, an exciton transfer length of 2.5 ± 0.5 μm has been reported.[16,17] This value is the longest yet reported for a perylene diimide derivative. The increased ordering of the perylene derivative film after vapor annealing also stabilizes charge-separated states, which slows charge recombination.[18] Therefore, to increase the efficiency of organic p−n junction solar cells, it is useful to design highly ordered perylene derivatives. Liquid crystals possess the ability to self-organize spontaneously into highly ordered structures. Due to the spontaneous ordering of the molecules in the liquid crystalline phase, very highly ordered films can be obtained after the liquid crystalline film is cooled to a crystalline phase. Therefore, the use of liquid crystalline perylene derivatives in organic p−n junctions is a promising method to increase the efficiency of such a solar cell.

So far, only a few liquid crystalline perylene derivatives have been synthesized.[19−24] In this paper the detailed phase behavior is discussed of *N,N′*-dialkyl-3,4,9,10-perylenetetracarboxyldiimides (Figure 1, with $n = 7$ (**1**), 12 (**2**), and 18 (**3**)). The phase transitions were determined using differential scanning calorimetry (DSC) and polarized optical microscopy (POM). The three-dimensional ordering of these perylene derivatives is examined with X-ray diffraction.[25] The cell parameters found by the X-ray diffraction measurements have been used in molecular mechanics simulations to find the lowest energetically favorable packing of the molecules in the liquid crystalline phases. Together with UV/vis spectroscopy studies on evaporated thin films of the perylene derivative, these measurements and simulations provide a detailed picture of the average ordering of these molecules.

To determine the usefulness of these perylene derivatives as semiconducting materials, e.g., in organic solar cells, the mobility of charge in *N,N′*-dioctadecyl-3,4,9,10-perylenebiscarboximide (**3**) has been measured using the pulse-radiolysis time-resolved microwave conductivity (PR-TRMC) technique.[26−28] PR-TRMC measurements yield the sum of the positive and negative charge carrier mobilities, $\Sigma\mu_{TRMC} = \mu(+) + \mu(-)$. Electrons have, however, been found on the majority charge carriers in this type of material, and would therefore be expected to contribute predominantly to $\Sigma\mu_{TRMC}$. Because of the nanosecond time scale of monitoring and the gigahertz electric field frequencies used, the mobilities obtained are trap-free values associated with well-organized domains within the material.[1,2] The value of $\Sigma\mu_{TRMC}$ should therefore be close to the maximum mobility that could be obtained in a dc device with a monodomain of that particular material between the electrodes. Very good agreement between mobility values determined by PR-TRMC and by dc time-of-flight (TOF) measurements has in fact been found for the liquid crystalline phases of the mesomorphic discotic material hexa(hexylthio)triphenylene, which forms well-organized, interelectrode layers.[28]

Experimental Details

Materials. The three perylene derivatives were synthesized on a 1 g scale by condensation of 3,4,9,10-perylenetetracarboxylic dianhydride with the corresponding amines according to the procedure of Demmig and Langhals,[29] and dried at 90 °C under vacuum and in the presence of P_2O_5.

***N,N′*-Diheptyl-3,4,9,10-perylenebiscarboximide (1):** yield 89%; ^{1}H NMR δ 8.94−8.67 (m, 8H), 4.45 (t, $J = 7.4$ Hz, 4H), 2.01 (quin, $J = 7.6$ Hz, 4H), 1.61−1.35 (m, 16H), 0.94 (t, $J = 7.0$ Hz, 6H); ^{13}C NMR δ 163.70, 131.49, 129.83, 126.93, 40.97, 32.10, 39.37, 28.73, 27.61, 22.89, 14.14; IR (KBr) 2954, 2927, 2854, 1696, 1654, 1636, 1593, 1577, 1559, 1540, 1507, 1457, 1437, 1405, 1379, 1343, 1268, 1246, 1089, 853, 809, 793, 747, 729 cm^{-1}; $C_{38}H_{38}N_2O_4$ found C 77.47, H 6.43, N 4.83; calcd C 77.79 H 6.53, N 4.78.

***N,N′*-Didodecyl-3,4,9,10-perylenebiscarboximide (2):** yield 83%; ^{1}H NMR δ 8.57−8.25 (m, 8H), 4.42 (t, $J = 7.4$ Hz, 4H), 2.30 (quin, $J = 7.4$ Hz, 4H), 1.61−1.32 (m, 16H), 0.91 (t, $J = 7.0$ Hz, 6H); ^{13}C NMR δ 163.27, 131.03, 129.35, 126.41, 40.64, 31.86, 29.61, 29.44, 29.28, 28.38, 22.59, 13.81; IR (KBr) 2952, 2927, 2851, 1697, 1656, 1593, 1560, 1507, 1460, 1437, 1405, 1376, 1344, 1295, 1275, 1250, 1165, 1090, 1015, 955, 914, 849, 809, 795, 779, 747, 729 cm^{-1}; $C_{48}H_{58}N_2O_4$ found C 79.05, H 8.01, N 3.58; calcd C 79.30 H 8.04, N 3.85.

***N,N′*-Dioctadecyl-3,4,9,10-perylenebiscarboximide (3)**: yield 63%; ^{1}H NMR δ 8,71−8.78 (m, 8H), 4.46 (t, $J = 7.6$ Hz, 4H), 2.03 (quin, $J = 7.0$ Hz, 4H), 1.62−1.33 (m, 60H), 0.94 (t, $J = 7.0$ Hz, 6H); ^{13}C NMR δ 163.74, 131.54, 128.89, 127, 40.98, 32.23, 30.05, 29.80, 29.65, 28.75, 27.68, 22.95, 14.17; IR (KBr) 2957, 2924, 2848, 1697, 1656, 1593, 1507, 1464, 1438, 1405, 1379, 1343, 1257, 1246, 1175, 1160, 1090, 853, 809, 750, 726, 669 cm^{-1}; $C_{60}H_{82}N_2O_4$ found C 80.34, H 9.41, N 2.83; calcd C 80.49 H 9.23, N 3.13.

Sample Characterization. ^{1}H and ^{13}C NMR spectra were acquired using a 400 MHz Bruker Avance DPX 400 spectrometer at 90 °C in 100 atom % D pyridine-d_5. Fourier transform infrared (IR) measurements were performed with a BIO Rad FTS-7 spectrophotometer. DSC measurements were conducted using a Perkin-Elmer DSC 7 calorimeter.

(13) Leznoff, C. C. *Phthalocyanines, Properties and Applications*; VCH Publishers: New York, 1989; pp 1−54.
(14) Simon, J.; André, J.-J. *Molecular Semiconductors*; Springer-Verlag: Berlin, 1985; pp 73−254.
(15) Gregg, B. A. *J. Phys. Chem.* **1996**, *100*, 852−859.
(16) Gregg, B. A.; Sprague, J.; Peterson, M. W. *J. Phys. Chem. B* **1997**, *101*, 5362−5369.
(17) Adams, D. M.; Kerimo, J.; Olson, E. J. C.; Zaban, A.; Gregg, B. A.; Barbara, P. F. *J. Am. Chem. Soc.* **1997**, *119*, 10608−10619.
(18) Kazmaier, P. M.; Hoffmann, R. *J. Am. Chem. Soc.* **1994**, *116*, 9684−9691.
(19) Cormier, R. A.; Gregg, B. A. *Chem. Mater.* **1998**, *10*, 1309−1319.
(20) Schlichting, P.; Rohr, U.; Müllen, K. J. *Mater. Chem.* **1998**, *8*, 2651−2655.
(21) Pressner, D.; Göltner, C.; Spiess, H. W.; Müllen, K. *Acta Polym.* **1994**, *45*, 188−195.
(22) Göltner, G.; Pressner, D.; Müllen, K.; Spiess, H. W. *Angew. Chem.* **1993**, *105*, 1722−1724.
(23) Müller, G. R. J.; Meiners, C.; Enkelmann, V.; Geerts, Y.; Müllen, K. J. *Mater. Chem.* **1998**, *8*, 61−64.
(24) Rohr, U.; Schlichting, P.; Böhm, A.; Gross, M.; Meerholz, K.; Bräuchle, C.; Müllen, K. *Angew. Chem., Int. Ed. Engl.* **1998**, *37*, 1434−1437.
(25) Mabis, E. J. *Acta Crystallogr.* **1962**, *15*, 1152−1157.
(26) Warman, J. M.; de Haas, M. P. In *Pulse Radiolysis*; Tabata, Y., Ed.; CRC Press: Boca Raton, FL, 1991; pp 101−133.
(27) Schouten, P. G.; Warman, J. M.; de Haas, M. P. *J. Phys. Chem.* **1993**, *97*, 9863−9870.
(28) Van de Craats, A. M.; Warman, J. M.; de Haas, M. P.; Adam, D.; Simmerer, J.; Haarer, D.; Schuhmacher, P. I. *Adv. Mater.* **1996**, *8*, 823−826.
(29) Demmig, S.; Langhals, H. *Chem. Ber.* **1988**, *121*, 225−230.

A 10 °C/min heating or cooling rate was used, and a nitrogen purge was maintained over the samples during the measurements. Transition temperatures were taken from the maximum points on the endotherms, and the enthalpies from the integrated area under the curves of the second heating run. For compound **1** transition temperatures and enthalpies were taken from the first heating run. Due to experimental limitations regarding the maximum temperature at which these measurements could be performed, it was not possible to measure a reproducible heating curve of **1**.

POM was performed on an Olympus BH-2 microscope equipped with a Mettler FP82HT hot stage and FP80HT temperature controller. The heating/cooling rate was 10 °C/min. Close to the transition temperatures observed with DSC, the heating and cooling rate was manually reduced to about 1 °C/min. X-ray diffraction measurements were performed using wide-angle X-ray scattering on a Siemens reflection diffractometer D5000 with an HTK oven and Cu Kα radiation.

Molecular Modeling. Molecular mechanics simulations of the three-dimensional ordering of **3** were performed with the MSI-program Cerius^2 (version 3.8),[30] using the "Smart Minimizer" energy minimization routine as implemented in the software. All structures were optimized in high-convergence mode with the PCFF force field.[31] This force field is an extended version of the consistent force field, CFF91,[32] and was used as available in the Cerius^2 program without modification. In all calculations, a preoptimized structure of **3** with both octadecyl chains in an all-trans conformation was placed in a unit cell with the dimensions as determined from the X-ray diffraction measurements. This unit cell was copied in the *a*, *b*, and *c* directions to produce a cluster of perylene molecules, each placed in a unit cell with the proper dimensions. In all computations this new unit cell was optimized with periodic boundary conditions in three dimensions, to prevent edge effects. During the optimizations all cell parameters, i.e., both cell lengths and angles (all at 90°), were fixed. Further details are given in the text.

UV/Vis Spectroscopy. All solvents used were of analytical grade and used without further purification, unless stated otherwise. Compound **1** was incorporated in a polyethylene matrix by placing polyethylene sheets in a 2.5 mM solution of **1** in 1,2,4-trichlorobenzene (Merck, zur synthese, 98%) at a temperature of 70 °C for 0.5 h and allowing them to swell. Several other solvents, i.e., chloroform and chlorobenzene, were tried as well; however, the spectra obtained for these sheets indicated the presence of aggregates of **1**. After swelling, the sheets were rinsed with 1,2,4-trichlorobenzene, followed by evaporation of the solvent and drying in air at room temperature for 3 days. The polyethylene sheets were stretched up to 5 times their original length using a homemade device.

Thin films of **3** with a layer thickness of about 40 nm were prepared by vacuum evaporation at $p \approx 10^{-5}$ Torr from a resistively heated molybdenum crucible onto quartz slides (Suprasil, 22 × 22 × 1 mm). Before deposition, the slides were thoroughly rinsed with 2-propanol and deionized water and blown dry with nitrogen.

Absorption spectra between 350 and 650 nm were recorded using a Cary 5E (Varian) spectrophotometer. For stretched polyethylene sheets polarized absorption spectra were obtained by placing a Glan-Taylor polarizer and a depolarizer in the sample beam before and after the sample, respectively. Spectra were corrected for the absorption of the polyethylene matrix. To measure spectra of the films, the spectrophotometer was equipped with an integrating diffuse reflectance sphere (Labsphere, DRA-CA-50), samples being positioned in the center of the sphere. Polarized absorption spectra in this case were obtained by placing sheet polarizers (Polaroid, type HNP′B) in the sample and reference beams.

PR-TRMC Technique. Using the PR-TRMC technique, a low concentration (ca. 10 μM) of electron−hole pairs is produced uniformly throughout the material by a nanosecond duration pulse of 3 MeV electrons from a Van de Graaff accelerator. This procedure, referred to as "radiation doping", does not perturb the primary molecular or higher order structure of the material. If the charge carriers formed are mobile, an increase in conductivity will occur which is monitored with nanosecond time resolution as a decrease in the power level of microwaves that traverse the sample. From the change in the microwave power level the radiation-induced conductivity of the medium at the end of the pulse, $\Delta\sigma_{eop}$, can be determined. This is related to the concentration of charge carrier pairs formed, N_p, and the sum of the mobilities, $\Sigma\mu_{TRMC} = \mu(+) + \mu(-)$, via

$$\Delta\sigma_{eop} = eN_p\Sigma\mu_{TRMC} \quad (1)$$

where *e* is the elementary charge. The concentration of charge carriers formed can be calculated from the amount of energy dissipated in the sample, which is accurately known from dosimetry, and the average energy required to produce one electron−hole pair, which can be estimated. The value of $\Sigma\mu_{TRMC}$ can then be determined from the measured value of $\Delta\sigma_{eop}$.

The experimental equipment and conditions and method of data analysis have been described in detail in previous publications.

Because of the ultrashort time scale of the measurements, charge carriers are usually observed before they recombine or have time to become localized at chemical (e.g., O_2) or physical (e.g., interfacial) defects. The measured mobility can therefore be considered to be "trap free". The use of microwaves to probe the conductivity change has the advantage over dc techniques that complications due to electrode contacts, space charge, and domain or grain boundaries are absent. Since trapping and interfacial barriers invariably result in a decrease in the effective mobility, the value of $\Sigma\mu_{TRMC}$ should be close to the maximum mobility that could possibly be obtained in a dc drift experiment with a single, well-organized monodomain of the material between the electrodes.

Well-organized layers with a thickness of tens of micrometers required for TOF measurements are not readily realized for the types of compounds studied in the present work. The discotic compound hexa(hexylthio)triphenylene (HHTT) has however been found to fulfill these requirements, and well-defined, Gaussian drift times have been determined for holes in this material in TOF measurements.[33] The mobilities derived from the TOF measurements in the mesophases of HHTT are found to be in very good agreement with the values derived from PR-TRMC measurements on the same material. TOF mobilities determined for other triphenylene derivatives are invariably lower than expected on the basis of the $\Sigma\mu_{TRMC}$ values presumably due to a lower degree of order within these materials.[26,34−36]

It should be pointed out that the mobility determined in PR-TRMC experiments corresponds to a random distribution of domain orientations within the bulk sample. For materials that are anisotropic the average mobility measured will be $(\mu_x + \mu_y + \mu_z)/3$. In the case of discotics the mobility is expected to be highly anisotropic with by far the highest mobility along the cores of the columnarly stacked aromatic macrocycles. This one-dimensional, intracolumnar mobility for this type of material will therefore be related to $\Sigma\mu_{TRMC}$ by $\Sigma\mu_{1D} = 3\Sigma\mu_{TRMC}$. Due to the large anisotropy, the mobility for discotic materials will depend on the orientation of the axis of the columnar stacks with respect to the electric field vector in a two-electrode, dc configuration, even with a well-ordered interelectrode layer. For parallel alignment a maximum mobility close to $3\Sigma\mu_{TRMC}$ would be expected. For a perpendicular orientation the mobility would be expected to be orders of magnitude lower. Any misorientation will therefore result in an even lower value of the mobility in a dc configuration than measured by PR-TRMC.

(30) Cerius2, version 3.8, Molecular Simulations Inc., 1998.

(31) (a) Sun, H. *Macromolecules* **1995**, *28*, 701−712. (b) Sun, H.; Mumby, S. J.; Maple, J. R.; Hagler, A. T. *J. Phys. Chem.* **1995**, *99*, 5873−5882. (c) Hill, J.-R.; Sauer, J. *J. Phys. Chem.* **1994**, *98*, 1238−1244.

(32) (a) Maple, J. A.; Hwang, M. J.; Stockfisch, T. P.; Dinur, U.; Waldman, M.; Ewig, C. S.; Hagler, A. T. *J. Comput. Chem.* **1994**, *15*, 162−182. (b) Hwang, M. J.; Stockfisch, T. P.; Hagler, A. T. *J. Am. Chem. Soc.* **1994**, *116*, 2515−2525.

(33) Adam, D.; Schuhmacher, P.; Simmerer, J. Häussling, L.; Siemensmeyer, K.; Etzbach, K. H.; Ringsdorf, H.; Haarer, D. *Nature* **1994**, *371*, 141−143.

(34) Warman, J. M.; Schouten, P. G. *J. Phys. Chem.* **1995**, 99, 17181−17185.

(35) Van de Craats, A. M.; de Haas, M. P.; Warman, J. M. *Synth. Met.* **1997**, *86*, 2125−2126.

(36) Van de Craats, A. M.; Siebbeles, L. D. A.; Bleyl, I.; Haarer, D.; Berlin, Y. A.; Zharikov, A. A.; Warman, J. M. *J. Phys. Chem. B* **1998**, *102*, 9625−9634.

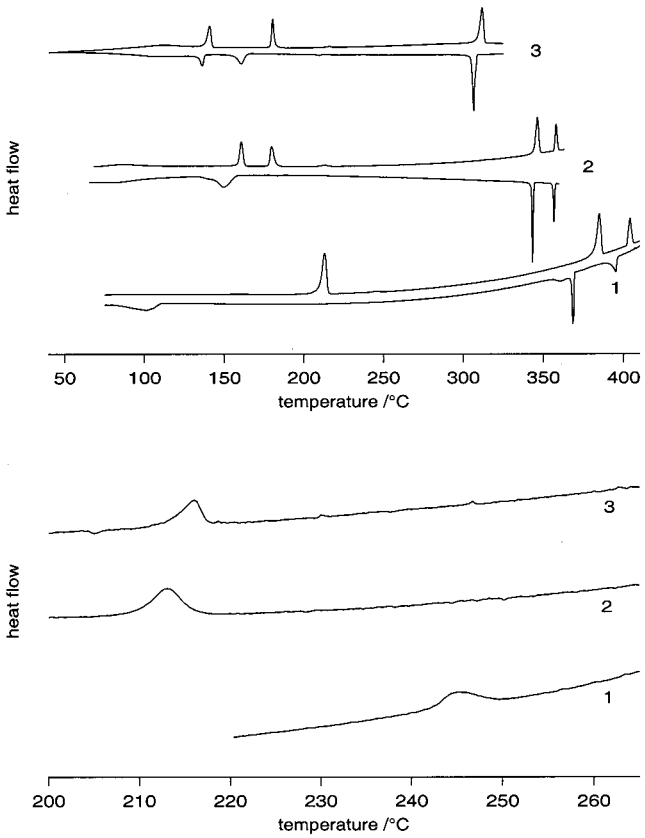

Figure 2. Top: DSC thermograms of compounds **1**−**3**. For **2** and **3** the second heating and cooling scans are given. For **1** the first heating and cooling scans are given. Bottom: Enlargement of the heating curves, which shows the phase transitions from $S_{x,1}$ to $S_{x,2}$ with a small enthalpy change.

Table 1. Phase Transition Temperatures (°C) (Corresponding ΔH Values (kJ/mol)) As Determined by DSC and Phase Types[a]

compd	transition temperatures
1[b,c]	K_1 213 (24.3)−LC_1 245 (0.5)−LC2 385 (21.8)−LC_3 404 (8.8)−I[c]
2[d]	K_1 87 (6.8)−K_2 161 (14.4)−K_3 180 (13.8)−$S_{x,1}$ 213 (1.2)−$S_{x,2}$ 346 (20.1)−LC 358 (9.4)−I
3[d]	K_1 111 (16.4)−K_2 141 (18.4)−K_3 180 (15.5)−$S_{x,1}$ 216 (0.9)−$S_{x,2}$ 312 (30.7)−I

[a] K = crystalline phase; S_x = highly ordered liquid crystalline phase (see the text); I = isotropic phase; LC = liquid crystalline phase, not characterized by X-ray. [b] Determined from the first heating. [c] As the phase transitions of **1** occur at slightly higher temperatures than those of **2** and **3**, extensive characterizations of the phases and phase transitions by POM and X-ray measurements were not possible, although these are likely in analogy to **2** and **3**. [d] Determined from the second heating scan.

This effect operates therefore in the same, negative direction as effects due to trapping and interfacial boundaries mentioned above.

Results and Discussion

Differential Scanning Calorimetry, Polarized Optical Microscopy, and X-ray Diffraction. The phase behavior of compounds **1**−**3** (Figure 1) was investigated with DSC, POM, and X-ray diffraction measurements. The DSC thermograms of the three perylene derivatives are depicted in Figure 2. Table 1 summarizes the phase transition temperatures and corresponding enthalpy changes, ΔH. Due to experimental limitations at high temperatures, it was not possible to measure a reproducible heating curve of **1**, as the isotropization temperature is >375 °C. The DSC scans of **2** and **3** do not change with subsequent heating and cooling starting from the first heating scan. From POM measurements it can be concluded that the peaks at 358 and 312 °C, for compounds **2** and **3**, respectively, are the isotropization phase transitions. With POM no changes were observed for any of the other phase transitions for all three perylene derivatives, which indicates that the relative orientation of the chromophores is approximately the same for all phases. From the DSC thermograms (Figure 2) it can be concluded that shortening of the alkyl chains results in an increase in isotropization temperature. This effect is also found for polyoxyethylene-substituted 3,4,9,10-perylenebiscarboximides.[19]

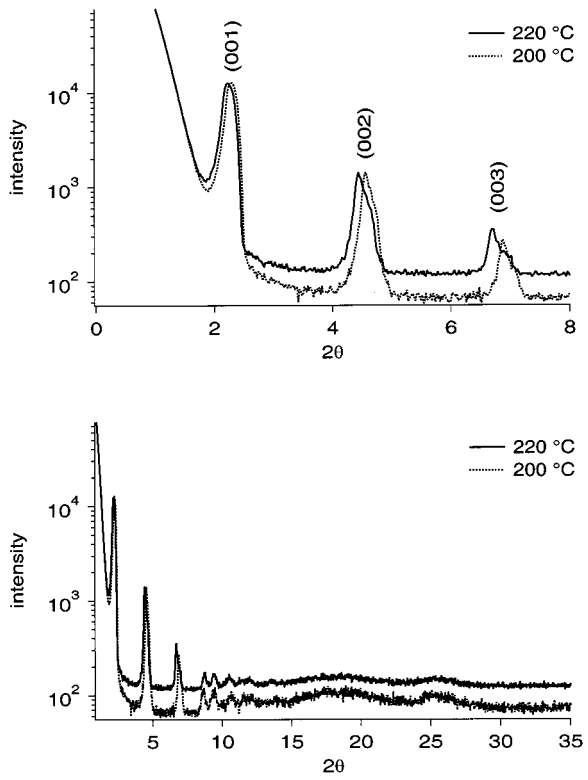

Figure 3. X-ray diffraction pattern of **3** at 200 and 220 °C (bottom), with enlarged (00*l*) reflections of **3** at 200 and 220 °C (top).

As the phase transitions of compound **3** occurred at lower temperatures than those of **1** and **2**, compound **3** was further examined by X-ray diffraction measurements. At the DSC-observed phase transition temperature changes also occurred in the X-ray diffraction pattern. A large number of sharp reflections was found at temperatures slightly above and below the first two-phase transitions (at 111 and 141 °C), indicating the occurrence of crystalline−crystalline phase transitions. At 180 °C, the halos, observable in the X-ray diffraction pattern, become more diffuse, which indicates the transition to a liquid crystalline phase. At 216 °C another phase transition occurs, and Figure 3 shows the X-ray diffraction pattern of **3** around this transition at 200 and 220 °C. First we discuss the X-ray diffraction pattern as observed for the second liquid crystalline phase at 220 °C, and then we will discuss the X-ray diffraction pattern at other temperatures: in the first liquid crystalline phase at 200 °C, and in the isotropic phase (400 °C).

With Bragg's law, the *d* spacing (d_{hkl}) can be calculated by using the measured diffraction angle. For a monoclinic cell the cell parameters *a*, *b*, and *c* were calculated—using eq 2,

$$d_{hkl} = \left[\frac{\frac{h^2}{a^2} + \frac{l^2}{c^2} + \frac{2hl\cos\beta}{ac}}{\sin^2\beta} + \frac{k^2}{b^2}\right]^{-0.05} \qquad (2)$$

Table 2. Experimental and Calculated Bragg Peaks and the Corresponding Miller Indices Used for Calculating the Dimensions of the Unit Cell at 220 °C

exptl Bragg peak/Å	calcd Bragg peak/Å	Miller indices	exptl Bragg peak/Å	calcd Bragg peak/Å	Miller indices
39.7	39.68	(001)	8.3	8.56	(102)
19.9	19.84	(002)	7.4	7.55	(103)
13.2	13.23	(003)	5.0	5.08	(200)
10.2	10.17	(100)	4.6	4.53	alkyl groups
9.5	9.52	(101)	3.6	3.60	(010)

Table 3. Dimensions of the Cell of **3** at Two Temperatures (200 and 220 °C) As Determined with X-ray Diffraction

temp (°C)	*a*/Å	*b*/Å	*c*/Å	β
200	10.3	3.6	39.0	82.5
220	10.3	3.6	40.1	81.7

which holds for monoclinic cells—by minimization of the error between the experimental and calculated values of the Bragg reflections.[37,38] Together with the corresponding Miller indices at 220 °C, these experimental and calculated values are presented in Table 2. The Miller indices were assigned via a trial and error process, and subsequent refinement of the parameters (using an Excel spreadsheet to minimize the sum of squares, with *a*, *b*, *c*, and θ as the parameters). The identification of the *c* axis is rather clear with three nicely spaced reflections reminiscent of higher ordered smectics ((001), (002), and (003)). The peak at 3.5 Å is as expected for the $\pi-\pi$ stacking distance (cf. discotics), and considering its relative sharpness compared to peaks from isotropic and nematic samples, the identification of this peak as (010) is also clear. The only remaining molecular dimension is the width of the aromatic groups in the 8−10 Å region. Using a spacing of 10 Å combined with a coupling to the *c* axis ((100), (101), (102), (103), and (200)), the remaining peaks can be explained. As can be seen, a good agreement exists between measured and fitted data, which lends strength to our assignment. Therefore, eq 2 was used to calculate the dimensions of the unit cell on the basis of the observed reflections, and the resulting values are listed in Table 3.

From the size of a single molecule of **3** (Figure 4) and the cell parameters from X-ray measurements (Table 3), a structural model for the intermolecular ordering at 220 °C can be derived, which is presented in Figure 5. In one dimension a layered (smectic) ordering is found: the layer of perylene cores is separated from the next layer of perylene cores by the alkyl chains. If the alkyl chain is all-trans, compound **3** is about 59.4 Å long. As the largest cell parameter is only 40.1 Å, the alkyl chains must be interdigitated. Three higher-order reflections are found for the layer−layer distances (39.7, 19.9, and 13.2 Å), which means that there exists a very regular repetition of these layers, despite the fact that this is solely based on the noncovalent interactions. Within the layers a two-dimensional order is observed. The cell parameter of 3.6 Å originates from the $\pi-\pi$ stacking of neighboring, cofacially stacked perylene cores, which results in the formation of columnar stacks.[39,40] In the X-ray diffraction pattern, the $\pi-\pi$ stacking gives a broad peak, which indicates that at 220 °C the columns are slightly

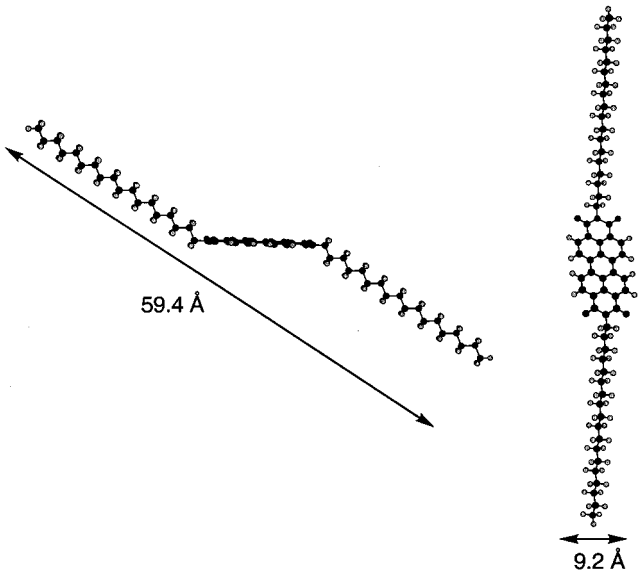

Figure 4. Relevant dimensions of compound **3**.

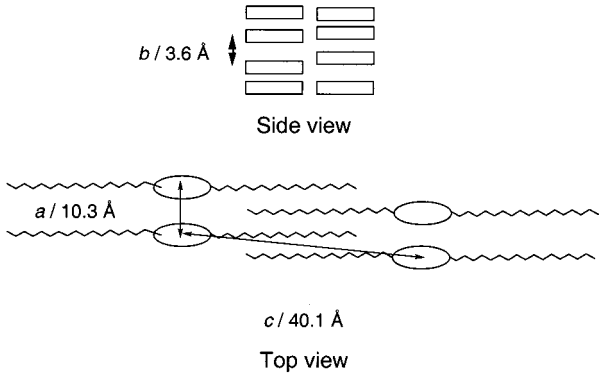

Figure 5. Schematic representation of the ordering of **3** at 220 °C according to X-ray diffraction patterns.

disordered and can slide past each other.[25] (This observation will be discussed in more detail later on, in combination with UV/vis spectroscopy and molecular mechanics data.) The cell parameter *a* is 10.3 Å, which is close to the perylene core width of 9.2 Å. This suggests that the most probable ordering of the perylene cores is edge-to-edge as depicted in Figure 5, top view.

The reflections found at 8.3, 7.4, and 4.6 Å correspond to Miller indices (102), (103), and (203), respectively. These mixed reflections indicate that the ordering of smectic layers is correlated to the edge-to-edge ordering of the perylene cores. This is caused by two factors: (1) the electric dipole of the carbonyl groups on the diimide moiety, which hinders free movement of the perylene cores in the *a* direction and (2) the steric interactions between the alkyl chains and the elliptic shape of the molecule. Due to the large interdigitation, the alkyl chains work on each other like anchors, and the alkyl chains also determine the edge-to-edge distance of the perylene cores. Therefore, the distance between smectic layers, which is dependent on the degree of interdigitation, is correlated to the cell parameter *a*.

Thus, at 220 °C, **3** is highly ordered in three dimensions, although at this temperature it is a liquid crystalline material, rather than a solid. From the results discussed above an ordering of molecules as depicted in Figure 5 is proposed. This ordering of molecules shows the characteristics of both a smectic ordering and a columnar discotic ordering. Such an ordering resembles that found for perylene derivative **4** (see Figure 6 for the

(37) Klut, H. P.; Alexander, L. E. *X-ray Diffraction Procedures for Polycrystalline and Amorphous Materials, 2nd ed.*; Wiley: New York, 1974.
(38) Rosenthal, J. *J. Chem. Educ.* **1991**, *68*, 285.
(39) Pressner, D.; Göltner, C.; Spiess, H.-W.; Müllen, K. *Ber. Bunsen-Ges. Phys. Chem.* **1993**, *97*, 1362−1365.
(40) Hunter, C. A.; Sanders, J. K. M. *J. Am. Chem. Soc.* **1990**, *112*, 5525−5534.

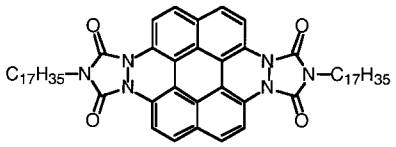

Figure 6. Structure of 4.[39]

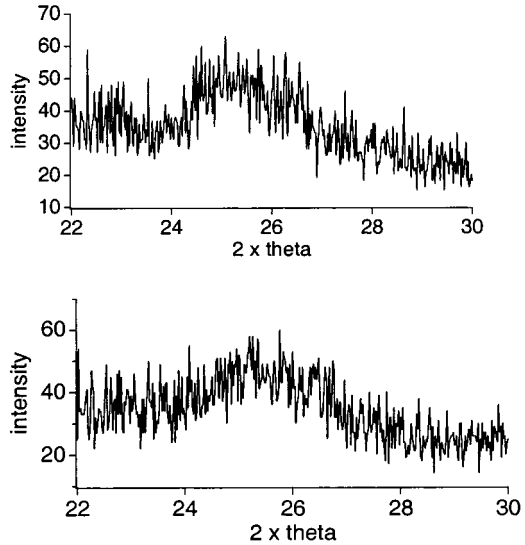

Figure 7. (010) reflections at 200 °C (top) and 220 °C (bottom).

molecular structure of this compound),[39] and can be denoted as a highly ordered mesophase, S_x.

Between 220 and 200 °C a phase transition occurs that shows up as a small peak in the DSC thermogram (Figure 2, bottom). From Figure 3 it can be seen that the X-ray patterns obtained at 200 and 220 °C differ only in two aspects, while the same Miller indices (not shown here) are found at both temperatures. First, the Bragg peaks that correspond to the (00*l*) reflections have shifted to a larger angle compared to that found at 220 °C (Figure 7). The shift of the (00*l*) reflection results in a smaller value for cell parameter *c*. Therefore, it can be concluded that in the lower temperature liquid crystalline phase, $S_{x,1}$, the alkyl chains are a little more interdigitated, by approximately one CH_2 unit. Second, the (010) reflection peak at 3.6 Å does not have a symmetric shape anymore. These (010) reflections at 200 and 220 °C are depicted in Figure 7. The asymmetric shape of this reflection at 200 °C indicates that the columns of perylenes slide past each other,[25] but the ordering within the columns is higher than in the $S_{x,2}$ phase at 220 °C, at which temperature the (010) reflection becomes symmetric. Thus, the small peak observed in the DSC diagram corresponds to a change in the interdigitation of the alkyl chains and a small change in order within the columns. Our data therefore show for the first time the presence of two clearly distinct, highly ordered, liquid crystalline phases that are both smectic *and* columnar discotic in nature.

X-ray measurements have also been performed on **2** at a temperature above the isotropization temperature (400 °C). In this X-ray diffraction pattern the (001) and (002) reflections were still present, indicating that a lamellar structure is preserved in the (macroscopically) isotropic phase, albeit with a smaller correlation length.

In Figure 5 the columns are rectangularly ordered with respect to the layered ordering. However, the experimental data do not exclude the possibility that the columns make an angle slightly different from 90° with respect to the layers.

Molecular Modeling. Molecular modeling can be a useful tool to investigate the packing structure and the columnar ordering of the perylene cores at 200 and 220 °C. With this technique a crystal structure can be mimicked by a unit cell, which is treated as a three-dimensionally repeating unit in the calculations.[41] This box should minimally be identical to the crystallographic unit cell, but optimally is a few times larger than this, to include all intermolecular interactions in an explicit and proper way in the computation.[42]

Preliminary investigations were done on a small unit cell containing only a few (six or nine) molecules of **3** to roughly determine the most favorable relative orientation of the molecules within a crystal structure. The relative orientation of these perylene diimides will be largely determined by a combination of interactions: $\pi-\pi$ interactions of aromatic groups within one stack, attractive and repulsive electrostatic interactions (e.g., between dipoles of adjacent diimide moieties within one stack, and those between diimide moieties in different stacks), and the van der Waals interactions between interdigitating alkyl chains. It was found in such small boxes that the molecules are ordered in perpendicular stacks (see Figure 5), and that the alkyl chains are highly interdigitated, which is as expected given the length of the unit cell (39.0 or 40.1 Å) compared to that of a fully stretched conformer of **3**, 59.4 Å.

The information obtained from these calculations was used to prepare two larger repeating boxes to better represent the experimental details.[42] These each consisted of 6 × 6 stacks of perylene molecules of **3**, using the cell parameters of the monoclinic cells as found with the X-ray diffraction measurements. Figure 8 presents the results for the cells fully optimized within the constraints of the cell parameters at 200 °C (Figure 8, structure **A**) and 220 °C (Figure 8, structure **B**).

In both structures the molecules form highly ordered structures with the perylene moieties in a discotic stack oriented along the *b* axis of the crystal cell. Five observations can be made for these perylene moieties: (a) The planes of the perylene rings within a discotic stack are oriented in a parallel fashion, with a nearly constant face-to-face distance (~3.6 Å) between the aromatic groups. (b) Every perylene is rotated by approximately 30° with respect to the molecules adjacent to it in the same stack around an axis that is perpendicular to the plane of the molecule (see Figure 8). This rotation is driven by optimization of dipole−dipole interactions between the diimide moieties in different layers, and the direction of this rotation seems to be random, also with respect to the neighboring layer (i.e., there is no indication for the formation of a chiral phase). (c) The center of mass of a perylene moiety is shifted by 1.5−2 Å with respect to the underlying molecule in a stack. In other words, in slight deviation from the schematic drawing in Figure 5, the calculated angle between the aromatic planes and the vector connecting the centers of mass of these molecules is somewhat smaller than 90° (on average 64°). This implies that the center-to-center distance is not 3.6 Å, but ca. 4 Å, which has implications for the expected exciton splitting (vide infra). (d) The length of the long axis of the unit cells seems to be determined by the balance between entropy and van der Waals attractions in the alkyl chains. This yields a significant interdigitation, which is nearly constant for both different molecules within one stack, and molecules from one stack to another. (e)

(41) For some recent examples see: (a) Galli, S.; Mercandelli, P.; Sironi, A. *J. Am. Chem. Soc.* **1999**, *121*, 1 (15), 3767−3772. (b) Chin, D. N.; Palmore, G. T. R.; Whitesides, G. M. *J. Am. Chem. Soc.* **1999**, *121*, 2115−2122. (c) Kudeva, S. S.; Craig, D. C.; Nangia, A.; Desiraju, G. R. *J. Am. Chem. Soc.* **1999**, *121 (9)*, 1936−1944. (d) Nakamura, M.; Tokumoto, H. *Surf. Sci.* **1998**, *398*, 143−153.

(42) (a) Sieval, A. B.; Van den Hout, B.; Zuilhof, H.; Sudhölter, E. J. R. *Langmuir* **2000**, 16, 2987−2990. (b) Barentsen, H. M.; Van Dijk, M.; Zuilhof, H.; Sudhölter, E. J. R. *Macromolecules* **2000**, 33, 766−774.

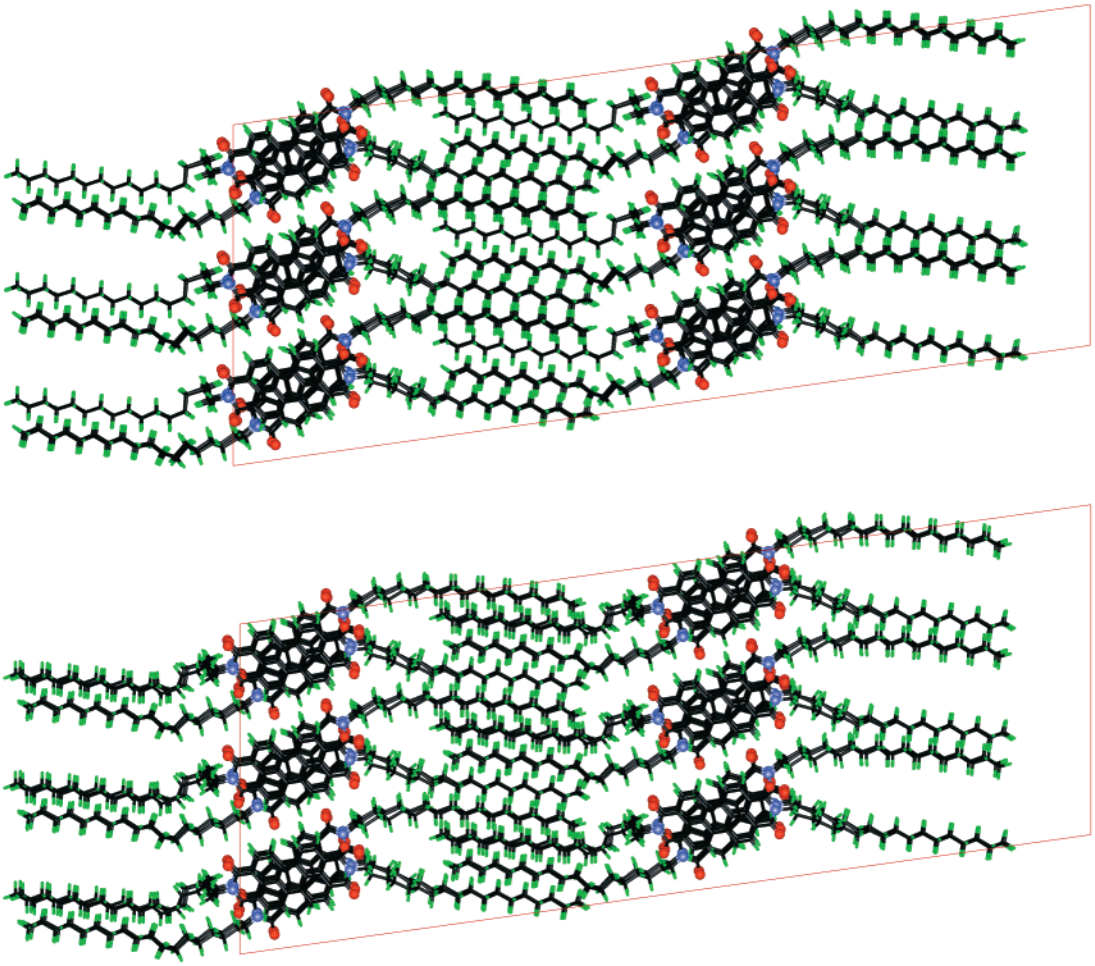

Figure 8. Three-dimensional packing of 3 as determined by PCFF molecular mechanics computations on a cluster of 36 perylene molecules in unit cells **A** (top) and **B** (bottom).

At lower temperatures the packing is somewhat tighter than at higher temperatures, which is displayed in the length of the unit cell (39.0 versus 40.1 Å at 200 and 220 °C, respectively). In line with this, structure **B** (220 °C) displays a slightly decreased interdigitation of these alkyl chains compared to structure **A** (200 °C). In addition, a marginal decrease in the order in the perylene stacks within box **B** is observed. Apparently, the extra space along the *c* axis that becomes thermally available in cell **B** compared to cell **A** is partially used to reduce the repulsion between the imide groups within a stack. The overall effect of the reduced repulsion and decreased degree of interdigitation at 220 °C compared to the situation at 200 °C yields a computed decrease in energy of 160 cal/mol per molecule in the box with 36 molecules. This tiny effect is in line with the experimental observation that the DSC signal in going from $S_{x,1}$ to $S_{x,2}$ is clear, but at the same time only very small (see enlargement in Figure 2).

UV/Vis Spectroscopy. To obtain information about the orientation of molecules in a condensed phase by optical spectroscopy, the orientation of the transition dipole moments in the molecular frame must be known. The molecular axis system used in this paper is represented in Figure 1. The perylene diimides (PTCDI) can be considered to belong to the D_{2h} symmetry point group, since their optical properties are determined by the π-electron system. This is confirmed by the fact that the absorption spectra in solution for many *N*-substituted PTCDI derivatives are virtually identical.[43−48] For planar aromatic molecules with D_{2h} symmetry, electric dipole allowed $\pi-\pi^*$ transitions can only be polarized in the *y* or *z* direction. For many planar aromatic hydrocarbons the lowest allowed optical transition is found to be polarized along the long in-plane symmetry axis of the molecule.[49] Deviations from pure *y* or *z* polarization can be observed if there are overlapping transitions or if a transition vibronically borrows intensity from another transition. In these cases, the dichroic ratio is generally found to be wavelength dependent.

The absorption spectra of **1**−**3** in chloroform are identical to that reported for **2**,[43] with maxima at 526, 490, 460, and 432 nm (see Figure 10). The spectrum of **1** in the matrix formed by the stretched polyethylene film is similar to that in chloroform except for a small red shift of about 2 nm, which is attributed to the different medium. For di-*tert*-butylphenyl-PTCDI, it has been shown that the absorption and emission dipoles are parallel along the whole vibronic progression and thus belong to a single electronic transition,[50] in line with calculations that also

(43) Icli, S.; Icil, H. *Spectrosc.* Lett. **1996**, 29, 1253; **1994**, 27, 323.
(44) Graser, F.; Hädicke, E. *Liebigs Ann. Chem.* **1980**, 1994.
(45) Sadrai, M.; Bird, G. R. *Opt. Commun.* **1984**, 51, 62.
(46) Rademacher, A.; Märkle, S.; Langhals, H. *Chem. Ber.* **1982**, 115, 2927.
(47) Gregg, B. A.; Sprague, J.; Peterson, M. W. *J. Phys. Chem. B* **1997**, 101, 5362.
(48) Lee, S. K.; Zu, Y.; Herrmann, A.; Geerts, Y.; Müllen, K.; Bard, A. J. *J. Am. Chem. Soc.* **1999**, 121, 3513.
(49) Michl, M.; Thulstrup, E. W. Spectroscopy with Polarized Light. Solute Alignment by Photoselection, in *Liquid Crystals, Polymers, and Membranes*; VCH Publishers: New York, 1986; Chapter 8.
(50) Johansson, L. B.-A.; Langhals, H. *Spectrochim. Acta* **1991**, 47A, 857.

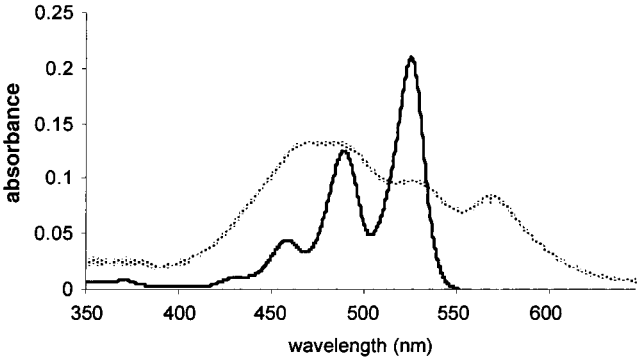

Figure 9. Absorption spectrum of a 10^{-5} M solution of **3** in chloroform (solid line) and of the evaporated **3** film (dashed line). The spectrum of **3** in solution is 5 times reduced.

predicted that the absorption bands are *z*-polarized.[51] To confirm the latter by experiment for the molecules under study, we performed polarized absorption measurements in stretched polyethylene sheets.

The dichroic ratio ($R_d = A_z/A_y$) for **1** in stretched polyethylene sheets was—within experimental error—found to be the same for all observed absorption bands and in agreement with the spectral anisotropy data of other PTCDI derivatives.[50] This indicates that also in this case the observed absorption is due to a single electronic transition. The dichroic ratio at infinite stretching $R_{d\infty}$ was derived from the experimentally obtained R_d values using the Tanazaki approximation,[52] yielding $R_{d\infty} = 7.5$. This implies an angle of $27 \pm 5°$ between the transition dipole moment and the orientation axis, similar to data found for perylene,[53,54] pentacene,[55] and other elongated aromatic molecules in polymer matrixes. These angles deviate from zero due to specific interactions of these aromatic molecules with the polymer matrix. Obviously these interactions dominate over the oblong molecular shape, which favors an angle of 0°. The alkyl chains in **1**, however, will most likely still be oriented in the stretch direction, since in the all-trans conformation they make an angle of ~30° with the PTCDI plane. From the value of $R_{d\infty} = 7.5$ it is therefore concluded that the transition dipole moment of the observed transitions in this D_{2h} molecule is oriented along the *z* axis of the PTCDI part of the molecule. Using this information, semiquantitative information about aggregate geometries can be obtained.

In Figure 9 the absorption spectrum of an evaporated film of **3** is also shown. In this spectrum four bands can be distinguished, at ~570, 530, 490, and 465 nm, the latter two of which are strongly overlapping. Compared to the solution spectrum, the film spectrum shows an additional red-shifted absorption band (at ~570 nm), which has also been observed for several other PTCDI derivatives.[44,56−62] These derivatives can roughly be divided into two classes: those with an absorption band at ~570 nm having a red color, and those that show absorption bands beyond 600 nm and have a black color. These differences have been ascribed to differences in the crystal structure[44] or to increased ordering of the film,[57−59] resulting in different degrees of π-overlap of adjacent molecules. For some PTCDI derivatives, transitions from the red to a black phase occur spontaneously[59,60] or after solvent vapor annealing.[57] The occurrence of such a transition is strongly dependent on the substituents attached to the aromatic core. Annealing of our films at higher temperatures or by solvent vapor annealing in CH_2Cl_2 vapor did not result in significant changes in the absorption spectrum. Polarized absorption spectra for the evaporated films did not show an anisotropy, in agreement with the POM measurements (vide supra). Since the observed spectral shift in the absorption spectrum clearly indicates strong interactions between the molecules, this means that the film probably consists of randomly oriented ordered domains that are much smaller than the illuminated area of about 0.5 cm^2.

The absorption bands observed for the film between 400 and 550 nm approximately coincide with those observed in the solution spectrum. The differences in intensity between the solution and film spectra in this region are not due to a different vibronic coupling for monomers in the film, as the spectra of PTCDIs in many different matrixes (solvents, polymers) are similar and thus relatively insensitive to environmental effects. We therefore conclude that also in this region the films show at least one additional absorption band at around 450 nm as compared to the solution spectrum. Therefore, the film spectra show two additional absorption bands, i.e., a blue-shifted band and a red-shifted band, upon going from (dilute) solution to film.

Spectral shifts observed upon aggregation of molecules are often explained using the point dipole model of Kasha.[63−65] According to this model, a shift of the absorption band to the red or the blue is expected if the transition dipoles involved are oriented in a parallel fashion, where the shift (blue or red) depends on the angle between the center-to-center vector and the transition dipole moments of the molecules. If the transition dipoles involved are not parallel, a blue-shifted absorption band *and* a red-shifted absorption band are expected simultaneously. Comparison of the spectra of the evaporated films with those of the monomer in solution shows both blue-shifted and red-shifted absorption bands (Figure 9). This phenomenon can be explained in two ways: (i) the transition dipole moments of adjacent PTCDI molecules are rotated with respect to each other (see the top view of perylene stacks in Figure 8) and/or (ii) more than one type of aggregate is present, with different orientations of adjacent molecules within the film. On the basis of the regularities observed in the X-ray spectra, in combination with the molecular dimensions, we can exclude the occurrence of a significant fraction of other types of aggregates. Therefore, a significant rotation exists between the transition dipole moments of adjacent perylene diimide molecules within one stack. Given the conclusion that this transition dipole moment is oriented in the *z* direction, a more quantitative treatment of the relative orientation of adjacent aromatics can be given.

(51) Adachi, M.; Murata, Y.; Nakamura, S. *J. Phys. Chem.* **1995**, 99, 14240.
(52) Tanizaki, Y.; Kubodera, S. *J. Mol. Spectrosc*. **1967**, 24, 1.
(53) Tanizaki, Y.; Yoshinaga, T.; Hiratsuka, H. *Spectrochim. Acta* **1978**, 34A, 205.
(54) Thulstrup E. W.; Michl, J.; Eggers, J. H. *J. Phys. Chem.* **1970**, 74, 3868.
(55) Thulstrup, E. W.; Michl, J. *J. Am. Chem. Soc.* **1982**, 104, 5594.
(56) Popovic, Z. D.; Loutfy, R. O.; Hor, A.-M. *Can. J. Chem.* **1985**, 63, 134.
(57) Gregg, B. A. *J. Phys. Chem.* **1996**, 100, 852.
(58) Gregg, B. A.; Sprague, J.; Peterson, M. W. *J. Phys. Chem. B* **1997**, 101, 5362.
(59) Cormier, R. A.; Gregg, B. A. *J. Phys. Chem. B* **1997**, 101, 11004.
(60) Cormier, R. A.; Gregg, B. A. *Chem. Mater.* **1998**, 10, 1309.
(61) Lifshitz, E.; Kaplan, A.; Ehrenfreund, E.; Meissner, D. *J. Phys. Chem.* **1998**, 102, 967.
(62) Lifshitz, E.; Kaplan, A.; Ehrenfreund, E.; Meissner, D. *Chem. Phys. Lett.* **1999**, 300, 626.
(63) McRae, E. G.; Kasha, M. *J. Chem. Phys.* **1958**, 28, 721.
(64) Kasha, M.; Rawls, H. R.; Ashraf El-Bayoumi, M. *Pure Appl. Chem.* **1965**, 11, 371.
(65) Kasha, M. In *Spectroscopy of the Excited State;* Di Bartolo, B., Ed.; Plenum Press: New York, 1976; pp 337−363.

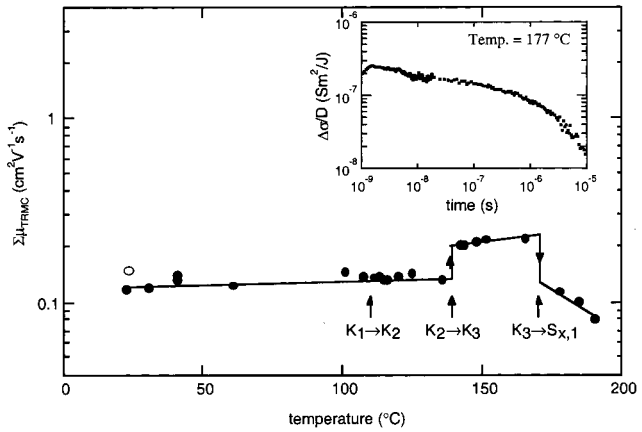

Figure 10. Temperature dependence of the pseudoisotropic charge mobility, $\Sigma\mu_{TRMC}$, in the octadecylperylene derivative **3**, determined by PR-TRMC. The filled circles are data for the first heating trajectory. The open circle is the value obtained after cooling back to room temperature. The inset shows a typical conductivity transient obtained for the liquid crystalline, $S_{x,1}$, phase using a 0.5 ns long electron pulse. Note the logarithmic time scale.

From the solution spectrum in Figure 9, a transition dipole moment of 7.4 ± 0.4 D was determined. Kasha's model can be used to estimate the exciton splitting, on the basis of the dielectric constant of the film (ca. 2) and geometrical properties of the complex. From X-ray diffraction and molecular modeling (vide supra) a center-to-center distance of ca. 4 Å was obtained, and angles of 64° between the center-to-center vector and the perylene plane and of 30° between the molecular transition dipoles. This yields a calculated exciton splitting of 0.4 eV, in excellent agreement with the observed value of ca. 0.4 eV. These results are therefore fully consistent with the calculated columnar ordering of cells **A**/**B**, i.e., an ordering in linear stacks but with alternately rotated molecules as indicated in Figure 8.

In previous studies it was concluded that Me-PTCDI films are built up from Me-PTCDI dimers or larger aggregates.[61,62] Our data are consistent with this, and this is also supported by the observation that films of **1**−**3** have the same color as the crystalline powders. Therefore, it can be concluded that also in the films large aggregates are formed. However, we can on the basis of our spectra not fully exclude the presence of a fraction of monomers in the films obtained from vacuum evaporation, as the absorption bands at 530 and 490 nm in the film spectrum approximately coincide with bands observed in the solution spectrum.

Pulse-Radiolysis Time-Resolved Microwave Conductivity. Readily measurable, long-lived conductivity transients were observed on pulsed irradiation of the octadecylperylene derivative **3** in its crystalline and liquid crystalline phases. An example of such a transient conductivity signal, obtained using a 0.5 ns pulse, is shown in Figure 10 (inset). The decay of the conductivity, due to the trapping and/or recombination of mobile charge carriers, is seen to occur on a time scale of hundreds of nanoseconds to microseconds, i.e., much longer than the pulse length.

The value of the charge mobility, $\Sigma\mu_{TRMC}$, was determined from the end-of-pulse conductivity as described in the Experimental Section. This is plotted as a function of temperature in Figure 10 for the first heating run on a freshly prepared powder sample starting at room temperature. No prior annealing or other sample conditioning was performed. The mobility of 0.12 $cm^2\ V^{-1}\ s^{-1}$ found at room temperature does not change significantly on heating until the K_3 phase is entered at 142 °C. At this phase transition the mobility undergoes an abrupt increase to 0.21 $cm^2\ V^{-1}\ s^{-1}$. A slight increase in mobility with a further increase in temperature occurs until at 177 °C the first mesophase is entered and $\Sigma\mu_{TRMC}$ suddenly drops to 0.11 $cm^2\ V^{-1}\ s^{-1}$. On further increasing the temperature in the mesophase, the mobility decreases to 0.08 $cm^2\ V^{-1}\ s^{-1}$ at the maximum temperature at which PR-TRMC measurements could be carried out, 190 °C. On cooling the sample from the liquid crystalline phase, the mobility returned to close to its initial room-temperature value.

The value of 0.11 $cm^2\ V^{-1}\ s^{-1}$ for $\Sigma\mu_{TRMC}$ in the liquid crystalline phase of **3** is close to the maximum values previously determined for other discotic materials, including derivatives of large macrocycles such as phthalocyanine and hexabenzocoronene.[28,66−68] As for the latter compounds, the migration of electronic charge is almost certainly mediated in compound **3** by the overlapping π-systems within the columnar stacks of aromatic cores. The high charge carrier mobility for the present imidoperylene derivative can therefore be ascribed to a very stable columnar arrangement of closely packed aromatic macrocycles in both the crystalline solid and liquid crystalline phases. This is in agreement with the columnar arrangement determined on the basis of the X-ray diffraction data. Because of this, the mobility is expected to be highly anisotropic with the largest component in the direction of the columnar axis. The one-dimensional mobility in this direction is therefore expected to be approximately a factor of 3 higher than the measured pseudoisotropic value of 0.11 $cm^2\ V^{-1}\ s^{-1}$, i.e., $\Sigma\mu_{1D} \approx 0.3\ cm^2\ V^{-1}\ s^{-1}$.

The relatively small decrease in mobility at the transition from the crystalline phase to the liquid crystalline phase contrasts with results for other discotic materials such as triphenylenes, porphyrins, and phthalocyanines for which much larger decreases, by up to an order of magnitude, are found at such phase transitions.[28,34,35,66,69] It would appear that the structural integrity of the stacked aromatic cores of the present perylene derivative is relatively insensitive to melting of the side chains. This could possibly result from the highly polar nature of the imido groups that provide stronger intermolecular interactions between neighboring macrocycles.

As emphasized in the Experimental Section, the PR-TRMC technique does not allow the separate determination of the mobility of positive and negative charge carriers. Substantial evidence is to be found in the literature, however, which indicates that imido-substituted aromatic compounds are good electron transport materials. Much of this evidence is indirect and is based on the improved properties of photovoltaic devices[12,70] or light-emitting diodes.[2,71] More direct evidence for mobile electrons has been deduced from the electrical

(66) Schouten, P. G.; Warman, J. M.; de Haas, M. P.; van Nostrum, C. F.; Gelinck, G. H.; Nolte, R. J. M.; Copyn, M. J.; Zwikker, J. W.; Engel, M. K.; Hanack, M.; Chang, Y. H.; Ford, W. T. *J. Am. Chem. Soc.* **1994**, 116, 6880−6894.

(67) Van de Craats, A. M.; Schouten, P. G.; Warman, J. M. *EKISHO* **1998**, 2, 12−27.

(68) Van de Craats, A. M.; Warman, J. M.; Fechtenkötter, A.; Brand, J. D.; Harbison, M. A.; Müllen, K. *Adv. Mater.* **1999**, 11, 1469−1472.

(69) Schouten, P. G.; Warman, J. M.; de Haas, M. P.; Pan, H. L. *Nature* **1991**, 353, 736−737.

(70) (a) Yu, G.; Gao, J.; Hummelen, J. C.; Wudl. F.; Heeger, A. J. *Science* **1995**, 270, 1789−1791. (b) Wöhrle, D.; Tennigkeit, B.; Elbe, J.; Kreienhoop, L.; Schnurpfeil, G. *Mol. Cryst. Liq. Cryst.* **1993**, 228, 221−226. (c) Ferrere, S.; Zaban, A.; Gregg, B. A. *J. Phys. Chem. B* **1997**, 101, 4490−4493. (d) Halls, J. J. M.; Friend, R. H. *Synth. Met.* **1997**, 85, 1307−1308. (e) Dittmer, J. J.; Petritsch, K.; Marseglia, E. A.; Friend, R. H.; Rost, H.; Holmes, A. B. *Synth. Met.* **1999**, 102, 879−880. (f) Savenije, T. J.; Warman, J. M.; Barentsen, H. M.; Van Dijk, M.; Zuilhof, H. Sudhölter, E. J. R. *Macromolecules* **2000**, 33, 60−66.

(71) Strukelj, M.; Papadimitrakopoulous, F.; Miller, T. M.; Rothberg, L. J. *Science* **1995**, 267, 1969−1972.

characteristics of field-effect transistor (FET) devices in which the transport layer consisted of an imidoaromatic compound.[2] In that study an electron mobility of 1.5×10^{-5} cm^2 V^{-1} s^{-1} was estimated for a perylenetetracarboxylic diimido derivative. A mobility of ca. 10^{-5} cm^2 V^{-1} s^{-1} has also been estimated for the negative charge carrier in an imidoperylene derivative using the time-of-flight method.[72] A considerably higher FET mobility, closer to 10^{-4} cm^2 V^{-1} s^{-1}, has been found for a diimidonaphthalene compound, and in the same paper, a mobility as high as 3×10^{-3} cm^2 V^{-1} s^{-1} was reported for a related carboxylic dianhydride derivative of naphthalene.[73] In both FET and TOF studies, measurements with reversed polarity of the electric field indicated much lower mobilities for the positive charge carrier.

In the course of processing of the present paper, results have been reported of FET mobility measurements in thin layers of dialkyl-substituted derivatives of naphthalenetetracarboxylic diimide,[74] compounds with structures very similar to those of the perylene derivatives studied in our work. In the report of Katz et al. it is shown that by carefully controlling the structure and oxygen content of the films an electron mobility as high as 0.16 cm^2 V^{-1} s^{-1} can be achieved. Interestingly, this is very close to the value of $\Sigma\mu_{1D}$ obtained in the present work for compound **3**. These recent results therefore tend to verify our suggestion that the mobilities obtained using the PR-TRMC technique represent close to the maximum values which could be achieved in dc device structures. The results furthermore support the conclusion that electrons make a major contribution to the charge mobility measured in the present work, although a significant additional contribution from positive charge carriers cannot be excluded. The self-organizing and self-healing properties of the liquid crystalline phase found for the present compounds could prove to be important additional properties of these materials for the formation of well-organized thin layers for n-type device applications, particularly if liquid crystalline properties can be achieved at room temperature by the incorporation of suitable mesogenic groups.

Since the TRMC technique is incapable of differentiating the charge of the majority charge carrier responsible for the conductivity, it cannot be completely excluded that the main contribution stems from hole transport. If, however, the electron is indeed the major charge carrier, then it is clear that high-mobility electron-conducting layers consisting of imidoaromatics should be possible, providing that the organized domains of the materials investigated here can be extended by structural organization within devices. Thus, the PR-TRMC experiments show a high charge carrier mobility for **3**, which makes this material a promising candidate for electron-transporting materials in photovoltaic devices.

(72) Ranke, P.; Bleyl, I.; Simmerer, J.; Haarer, D.; Bacher, A.; Schmidt, H. W. *Appl. Phys. Lett.* **1997**, 71, 1332−1334.

(73) Laquindanum, J. G.; Katz, H. E.; Dodabalapur, A.; Lovinger, A. J. *J. Am. Chem. Soc.* **1996**, 118, 11331−11332.

(74) Katz, H. E.; Lovinger, A. J.; Johnson, J.; Kloc, C.; Siegrist, T.; Li, W.; Lin, Y.-Y.; Dodabapalur, A. *Nature* **2000**, *404*, 478−480.

Conclusions

Three *N,N′*-dialkylated 3,4,9,10-perylenetetracarboxyldiimides were synthesized, and their phase behavior was investigated. A combination of differential scanning calorimetry, polarized optical microscopy, and X-ray diffraction measurements showed for the first time the presence of two highly ordered liquid crystalline phases that are both smectic and columnar discotic in nature. Using a combination of molecular mechanics and UV/vis spectroscopy, it was deduced that the perylene moieties within a discotic column are rotated by ca. 30° in going from one layer to the other. The combination of the interdigitation of the linear alkyl chains, attractive $\pi-\pi$ interactions between the perylene moieties, and the strong dipolar interactions between the diimide moieties within one column and between adjacent columns results in the aforementioned highly ordered structure. PR-TRMC measurements show that compound **3** has a charge carrier mobility of 0.1 cm^2 V^{-1} s^{-1} in the liquid crystalline phase, and in the crystalline phase a charge carrier mobility as high as 0.2 cm^2 V^{-1} s^{-1}. This is comparable with the highest values previously found for other discotic materials. The combination of high structural order, excellent processability via the liquid crystalline phases, and high charge carrier mobility makes these materials promising candidates for an electron-accepting and electron-transporting layer in a variety of opto-electronic devices, such as an all organic solar cell.

Acknowledgment. We thank Prof. W. H. de Jeu (AMOLF) for his useful discussion on the X-ray diffraction measurements and Prof. J. Perlstein (University of Rochester) for extensive and clarifying discussions. We are grateful to the Netherlands Organization for Energy and Environment (NOVEM) for generous funding of this research.

JA000991G